Basic Research in Cardiology (2023) 118:35
https://doi.org/10.1007/s00395-023-01005-1

ORIGINAL CONTRIBUTION

Cardiac fibroblast GSK-3α aggravates ischemic cardiac injury by promoting fibrosis, inflammation, and impairing angiogenesis

Prachi Umbarkar[1] · Suma Ejantkar[1] · Sulivette Y. Ruiz Ramirez[1] · Angelica Toro Cora[1] · Qinkun Zhang[1] · Sultan Tousif[1] · Hind Lal[1]

Received: 30 May 2023 / Revised: 14 August 2023 / Accepted: 16 August 2023 / Published online: 1 September 2023

Abstract

Myocardial infarction (MI) is the leading cause of death worldwide. Glycogen synthase kinase-3 (GSK-3) has been considered to be a promising therapeutic target for cardiovascular diseases. GSK-3 is a family of ubiquitously expressed serine/threonine kinases. GSK-3 isoforms appear to play overlapping, unique, and even opposing functions in the heart. Previously, our group identified that cardiac fibroblast (FB) GSK-3β acts as a negative regulator of fibrotic remodeling in the ischemic heart. However, the role of FB-GSK-3α in MI pathology is not defined. To determine the role of FB-GSK-3α in MI-induced adverse cardiac remodeling, GSK-3α was deleted specifically in the residential fibroblast or myofibroblast (MyoFB) using tamoxifen (TAM) inducible Tcf21 or Periostin (Postn) promoter-driven Cre recombinase, respectively. Echocardiographic analysis revealed that FB- or MyoFB-specific GSK-3α deletion prevented the development of dilative remodeling and cardiac dysfunction. Morphometrics and histology studies confirmed improvement in capillary density and a remarkable reduction in hypertrophy and fibrosis in the KO group. We harvested the hearts at 4 weeks post-MI and analyzed signature genes of adverse remodeling. Specifically, qPCR analysis was performed to examine the gene panels of inflammation (TNFα, IL-6, IL-1β), fibrosis (COL1A1, COL3A1, COMP, Fibronectin-1, Latent TGF-β binding protein 2), and hypertrophy (ANP, BNP, MYH7). These molecular markers were essentially normalized due to FB-specific GSK-3α deletion. Further molecular studies confirmed that FB-GSK-3α could regulate NF-kB activation and expression of angiogenesis-related proteins. Our findings suggest that FB-GSK-3α plays a critical role in the pathological cardiac remodeling of ischemic hearts, therefore, it could be therapeutically targeted.

Keywords Glycogen synthase kinase · Myocardial infarction · Fibrosis · Angiogenesis · Inflammation

Introduction

Myocardial infarction (MI) is one of the major causes of mortality, leading to millions of deaths worldwide [49]. In most cases, MI happens as a result of thrombus formation in coronary arteries that leads to prolonged ischemia subsequently causing necrosis of cardiomyocytes (CMs). MI triggers a wound-healing response that comprises sequential activation of inflammatory, proliferative, and maturation phases [6, 8, 12, 17, 38]. In the injured myocardium, fibroblasts (FBs) undergo phenotypic changes and play critical roles in wound healing and remodeling [14, 20, 35, 46, 48]. The death of necrotic CMs activates the inflammatory phase in which leukocytes infiltrate infarcts and clear debris [13]. FBs acquire pro-inflammatory phenotype and participates in inflammation. The resolution of the inflammatory response is followed by the proliferation phase. During this phase, FBs get transformed into myofibroblasts (MyoFBs). MyoFBs and endothelial cells proliferate and participate in a new matrix formation, neo-vascularization, and scar formation. During scar maturation, FBs undergo apoptosis/revert to the quiescent stage/become matrifibrocytes. After wound healing, the heart undergoes structural and functional remodeling that offsets increased load, attenuates progressive dilatation, and maintains contractile function. However, pressure

✉ Prachi Umbarkar
pumbarkar@uabmc.edu

✉ Hind Lal
hindlal@uabmc.edu

[1] Division of Cardiovascular Disease, UAB|The University of Alabama at Birmingham, 1720 2nd Ave South, Birmingham, AL 35294-1913, USA

and volume overload in the remodeled heart may lead to activation of FBs and excessive fibrosis that may further aggravate the disease pathology. Considering the widespread role of FBs in post-MI healing and remodeling, better insights into FB-specific molecular signaling that underlie these processes could provide novel therapeutic targets to treat cardiac pathologies in MI patients.

GSK-3 is a family of ubiquitously expressed serine/threonine kinases. The GSK-3 family consists of two isoforms, GSK-3α and GSK-3β. The roles of GSK-3 isoforms have been extensively studied in the pathogenesis of cardiac diseases [4, 25, 51]. Since CMs are basic contractile units of the heart, most of these studies were designed to understand the CM-specific GSK-3 regulated mechanisms. Recent development in FB-specific genetic models, such as Tcf21-MCM and Postn-MCM, allowed us to perform genetic manipulation in FBs and have expanded our knowledge of the diverse roles of FBs in cardiac homeostasis and diseases [1, 23, 50]. Our lab has demonstrated that FB-specific GSK-3β acts as a negative regulator of fibrosis in the ischemic heart [26]. Specifically, deletion of GSK-3β from FBs leads to excessive fibrosis, profound scaring, dilative remodeling, and cardiac dysfunction in the infarcted heart. However, the role of FB-GSK-3α in MI pathogenesis is completely unknown. In the present study, we report that FB-specific deletion of GSK-3α before ischemic insult (Tcf21-MCM model) prevents MI-induced fibrosis and chronic inflammation, and improves angiogenesis. In a relatively more translational mode, we further confirm that deleting GSK-3α from activated FBs or MyoFBs after MI injury (Postn-MCM model) offers similar benefits.

Materials and methods

Mice

Resident fibroblast-specific GSK-3α KO (GSK-3α^{FKO}) and myofibroblast-specific GSK-3α KO (GSK-3α^{MFKO}) were generated as described previously [53]. The GSK-3α $^{fl/fl}$/Cre$^{+/-}$/TAM mice were denoted as fibroblast knockouts (GSK-3α^{FKO} or GSK-3α^{MFKO}), whereas littermates GSK-3α $^{fl/fl}$/Cre$^{-/-}$/TAM represented as controls (CTRL). A cohort of animals of both sexes was recruited to investigate the sex-specific effect of FB-GSK-3α deletion on MI pathology. We did not observe sex-specific differences in our models. No animals were excluded from the analysis. The Institutional Animal Care and Use Committee of the University of Alabama at Birmingham approved all animal procedures and treatments used in this study (protocol # IACUC-21701). Animal Research: Reporting in vivo Experiments (ARRIVE) guidelines were followed [41].

Coronary artery ligation surgery (myocardial infarction)

MI surgery was performed as described previously and guidelines recommended by the AJP-Heart and Circulatory Physiology for experimental models of MI were followed [15, 31]. Briefly, mice were anesthetized with isoflurane (1.5–2%), and analgesic (buprenorphine-SR, 0.5 mg/kg per body weight, subcutaneous) before surgery. The thoracotomy was performed to temporarily displace the heart from the cavity. A suture (6.0 silk) was placed 2 mm below the origin of the left anterior descending (LAD) coronary artery and occlusion was confirmed by visual blanching of the area. The heart was replaced immediately into the thoracic cavity, the air was evacuated, and the chest was closed. Sham surgery was performed exactly as described above but the LAD was not ligated.

Echocardiography

Echocardiography was performed as described previously [32, 52]. In brief, mice were anesthetized with isoflurane (1–1.5%), and transthoracic M-mode echocardiography was performed with a 12-MHz probe (VisualSonics). LV end-systolic interior dimension (LVID;s), LV end-diastolic interior dimension (LVID;d), ejection fraction (EF), and fractional shortening (FS) values were obtained by analyzing data using the Vevo 3100 program.

Histology

Heart tissues were fixed in 10% neutral buffered formalin, embedded in paraffin, and sectioned at 5 µm thickness. Sections were deparaffinized with xylene and rehydrated by incubating with decreasing concentrations of ethanol. For detection of fibrosis, sections were stained with Masson Trichrome (Sigma-Aldrich, #HT15) as per the manufacturer's instructions. The images of the LV region were captured using a Nikon Eclipse E200 microscope with NIS element software version 5.20.02. The quantification of LV fibrosis was determined with ImageJ version 1.52a software (NIH). For fibrosis measurement 8–10 images covering the LV region were taken, and LV fibrosis was quantified as a percentage of the total LV area scanned.

Immunofluorescence studies

For immunofluorescence studies, heart tissues were embedded in the OCT compound (Fisher Scientific, #23-730-571) and cryosectioned. Sections were air dried, washed with PBS, fixed with 4% paraformaldehyde (PFA) for 15 min

at RT, and incubated with FITC-conjugated Wheat germ agglutinin (WGA) (Invitrogen, #W834) for 30 min at RT in the dark. After staining sections were washed with PBS and mounted in ProLong Gold antifade reagent with DAPI (Invitrogen, #P36941). For CD31 staining, tissue sections were air dried, washed with PBS, fixed with 4% PFA for 15 min at RT, and permeabilized with 0.4% Triton X-100 in PBS (PBST) for 20 min. To block non-specific antibody binding, sections were incubated with a blocking solution (5% goat serum in PBST) for 30 min at RT. After blocking, sections were incubated overnight with CD31 antibody (1:50 dilution in PBST, BD Pharmingen, #550274) at 4 °C followed by secondary antibody (1:100 dilution in PBST, Invitrogen, #A11007) staining for 1 h at RT. Sections were mounted in ProLong Gold antifade reagent with DAPI (Invitrogen, #P36941). All fluorescent images were taken on a KEYENCE BZ-X800 fluorescence microscope. The quantification of the cross-sectional area of cardiomyocytes (CSA) and mean fluorescent intensity (MFI) of CD31 were determined with ImageJ version 1.52a software (NIH). At least 200–300 cardiomyocytes per heart ($n=5$ hearts per group) were taken for CSA measurement.

Fibroblasts isolation, cell culture, and treatments

Adult mouse cardiac fibroblasts

Adult mouse cardiac fibroblasts were isolated according to a previous protocol [53]. Briefly, hearts were excised and rinsed in cold Krebs–Henseleit (Sigma, #K7353) buffer supplemented with 2.9 mM $CaCl_2$ (Sigma, #C3306) and 24 mM $NaHCO_3$ (Sigma, #S5761). The tissue was minced and transferred to the Enzyme cocktail [0.25 mg/mL Liberase TH (Roche, #05401151001), 20 U/mL DNase I (Sigma Aldrich, #D4527), 10 mmol/L HEPES (Gibco, #15630-080), in HBSS (Cellgro, #21-023-CV)], and serial digestions were performed at 37 °C for 30 min. After each digestion, digests were passed through a 40 µm filter and collected in a tube containing DMEM-F12 with 10% FBS. At the end of the digestion protocol, cells were pelleted by centrifugation at 1000 rpm for 10 min. To remove RBCs, the cell pellet was re-suspended in 1 mL of RBC/ACK lysis buffer (Gibco, #A1049201) and incubated for 1 min. Following incubation, cells were washed with the KHB buffer and centrifuged at 1000 rpm for 10 min. Cells were re-suspended in DMEM-F12 with 10% FBS and plated into a 100 mm culture dish for 2 h. Unattached and dead cells were washed with DPBS, and fresh media was added to maintain fibroblast culture.

Mouse embryonic fibroblasts: MEFs

The creation of WT and GSK-3α KO MEFs used in this study have been described previously [11]. MEFs were grown in Dulbecco's Modified Eagle's medium (DMEM) supplemented with 10% FBS (GIBCO) and 1% penicillin–streptomycin (GIBCO). Cells were serum-starved overnight and treated with TNF-α (10 ng/mL; Sigma, #GF023) for 1 h.

Immunoblotting

Proteins were extracted from cells using cell lysis buffer (Cell Signaling Technology, #9803S) containing 50 mM Tris–HCl (pH7.4), 150 mM NaCl, 1 mM EDTA, 0.25% sodium deoxycholate, 1% NP-40, Protease Inhibitor Cocktail (Sigma-Aldrich #P8340) and Phosphatase Inhibitor Cocktail (Sigma-Aldrich, #P0044). Protein concentration was determined with the Bio-Rad Protein Assay Dye (Bio-Rad, #5000006) according to the manufacturer's instructions. An equal amount of proteins was denatured in SDS–PAGE sample buffer, resolved by SDS–PAGE, and transferred to the Immobilon-P PVDF membrane (EMD Millipore, #IPVH00010). The membranes were blocked in Odyssey blocking buffer (LI-COR Biosciences, #927-40000) for 1 h at RT. Primary antibody incubations were performed at different dilutions as described in the antibody list in Supplemental Table 1. All incubations for primary antibodies were done overnight at 4 °C and followed by secondary antibody (IRDye 680RD or IRDye 800CW from LI-COR Biosciences) incubation at 1:3000 dilutions for 1 h at RT. Recommended antibody use guidelines were followed [7]. Proteins were visualized with the Odyssey Infrared Imaging System (LI-COR Biosciences). Band intensity was quantified by Image Studio version 5.2 software. β-Tubulin was used as a loading control. The data are presented as fold change relative to the experimental control group. At 1 week post-MI, cardiac fibroblasts were isolated and cultured. Cells from passage-1 were harvested and Angiogenesis-related proteins were analyzed using the Proteome Profiler™ Array—Mouse Angiogenesis Array Kit (R&D Systems, #ARY015) as per the manufacturer's protocol. The average signal (Mean Pixel Intensity) was calculated using Image Studio version 5.2 software.

RNA extraction and quantitative PCR analysis

Total RNA was extracted using the RNeasy Mini Kit (Qiagen, #74104) according to the manufacturer's protocol. cDNA was synthesized using the iScript cDNA synthesis kit (Bio-Rad, #170-8891) following the manufacturer's instructions. Gene expression was analyzed by quantitative PCR (qPCR) using the TaqMan Gene Expression Master Mix (Applied Biosystems, #4369016) and TaqMan gene expression assays (Applied Biosystems) on a Quant studio 3 (Applied Biosystems) Real-Time PCR Detection machine. To confirm FB-specific deletion, adult mouse

cardiac fibroblasts were isolated from mice as described in the previous section. To enrich the FB population, endothelial (CD31+) and myeloid (CD45+) cells were sorted using the Magnetic Cell Isolation and Cell Separation kit (Miltenyi Biotec) with recommended dilutions of antibodies—CD31 (Miltenyi Biotec, #130-097-418) and CD45 (Miltenyi Biotec, #130-052-301) as per the manufacturer's instructions. After enrichment, RNA was extracted from FBs and used for gene expression analysis. Details of TaqMan gene expression assays used in this study are provided in Supplemental Table 2. Relative gene expression was determined by using the comparative CT method ($2^{-\Delta\Delta CT}$) and was represented as fold change. Briefly, the first ΔCT is the difference in threshold cycle between the target and reference genes: $\Delta CT = CT$ (a target gene X) − CT (18S rRNA) while $\Delta\Delta CT$ is the difference in ΔCT as described in the above formula between the CTRL and KO group, which is = ΔCT (KO target gene X) − ΔCT (CTRL target gene X). Fold change is calculated using the $2^{-\Delta\Delta CT}$ equation.

Statistical analysis

Randomization and blinding were carried out while performing experiments, data acquisition, and analysis. The statistical analyses were performed using GraphPad Prism (version 9.0.0). The Shapiro–Wilk test was used to determine the normality of data. For normally distributed data, 2-way ANOVA (for 2 variables) was conducted followed by Tukey post hoc analysis. In case of non-normal distribution, an unpaired 2-tailed Mann–Whitney test was used to compare 2 groups. Data are presented as means ± SD. *N* per group and statistical test used for analysis are reported in figure legends. A P value of < 0.05 was considered statistically significant.

Results

Deleting GSK-3α from resident cardiac fibroblast before injury prevents ischemia-induced cardiac dysfunction

To evaluate the role of resident fibroblast GSK-3α in injury-induced cardiac remodeling, we generated FB-specific GSK-3α KO mice as described previously [53]. Briefly, Tcf21-MCM mice were crossed with GSK-3α$^{fl/fl}$ mice to obtain GSK-3α$^{fl/fl}$/Tcf21-MCM$^{+/-}$ (KO) and GSK-3α$^{fl/fl}$/Tcf21-MCM$^{-/-}$ (CTRL). Tamoxifen protocol was employed 2 weeks before MI surgery and continued till the end point of the studies. After TAM treatment, FBs were isolated, and gene expression analysis was carried out to confirm FB-specific GSK-3α deletion (Fig. 1A and B). The qPCR results showed a 95% reduction in GSK-3α gene expression in KO FBs as compared to the control group. Mice were subjected to permanent LAD ligation and cardiac function was monitored by serial echocardiography. MI-induced mortality was comparable between the groups (data not shown). The CTRL-MI group showed a significant decline in EF and FS as compared to CTRL-SHAM, indicating the development of systolic dysfunction (Fig. 1C and D). This functional change was associated with dilative cardiac remodeling as evidenced by the significant increase in LVIDs (Fig. 1E and F). All these parameters were normalized in the KO-MI group, indicating that FB-specific GSK-3α is a key regulator of ischemic injury-induced dilative remodeling and cardiac dysfunction.

FB-specific deletion of GSK-3α prevents ischemia-induced cardiac hypertrophy and fibrosis

Prominent change in LVIDs prompted us to examine the effect of GSK-3α deletion on the ischemia-induced cardiac remodeling process. Morphometrics and histology studies were performed at 4 weeks post-MI. The heart weight to tibia length ratio (HW/TL) was examined to assess cardiac hypertrophy. As expected, the CTRL-MI group showed a significant increase in HW/TL compared to the CTRL-SHAM group (Fig. 2A). To examine hypertrophy at the cellular level, LV-sections were stained with FITC-conjugated wheat germ agglutinin (WGA), and cardiomyocyte cross-sectional areas were measured (CSA). In line with previous observations, the CTRL-MI group showed a remarkable increase in CSA, confirming CM hypertrophy in CTRL-MI hearts (Fig. 2B). To assess cardiac fibrosis Masson's Trichrome staining was carried out. We observed excessive replacement as well as interstitial fibrosis in the CTRL-MI group. All these pathological features of MI were mitigated in the KO-MI group (Fig. 2C). Additionally, qPCR analysis was carried out to compare expression levels of key genes related to cardiac hypertrophy (ANP, BNP, and MYH7) and fibrosis (COL1A1, Fibronectin, and LTBP-2). These molecular markers were significantly augmented in the CTRL-MI group but were normalized in KO-MI (Fig. 2D–I). Taken together, these findings confirmed that deletion of GSK-3α from resident FBs before ischemic injury attenuated adverse cardiac remodeling and improved cardiac function.

Deletion of GSK-3α from resident cardiac fibroblasts reduces chronic inflammation and promotes angiogenesis in the MI heart

Prolonged inflammation and impaired angiogenesis contribute to adverse cardiac remodeling and the development of cardiac dysfunction post-MI. Hence, we examined the effect of FB-GSK-3α deletion on these processes. Our

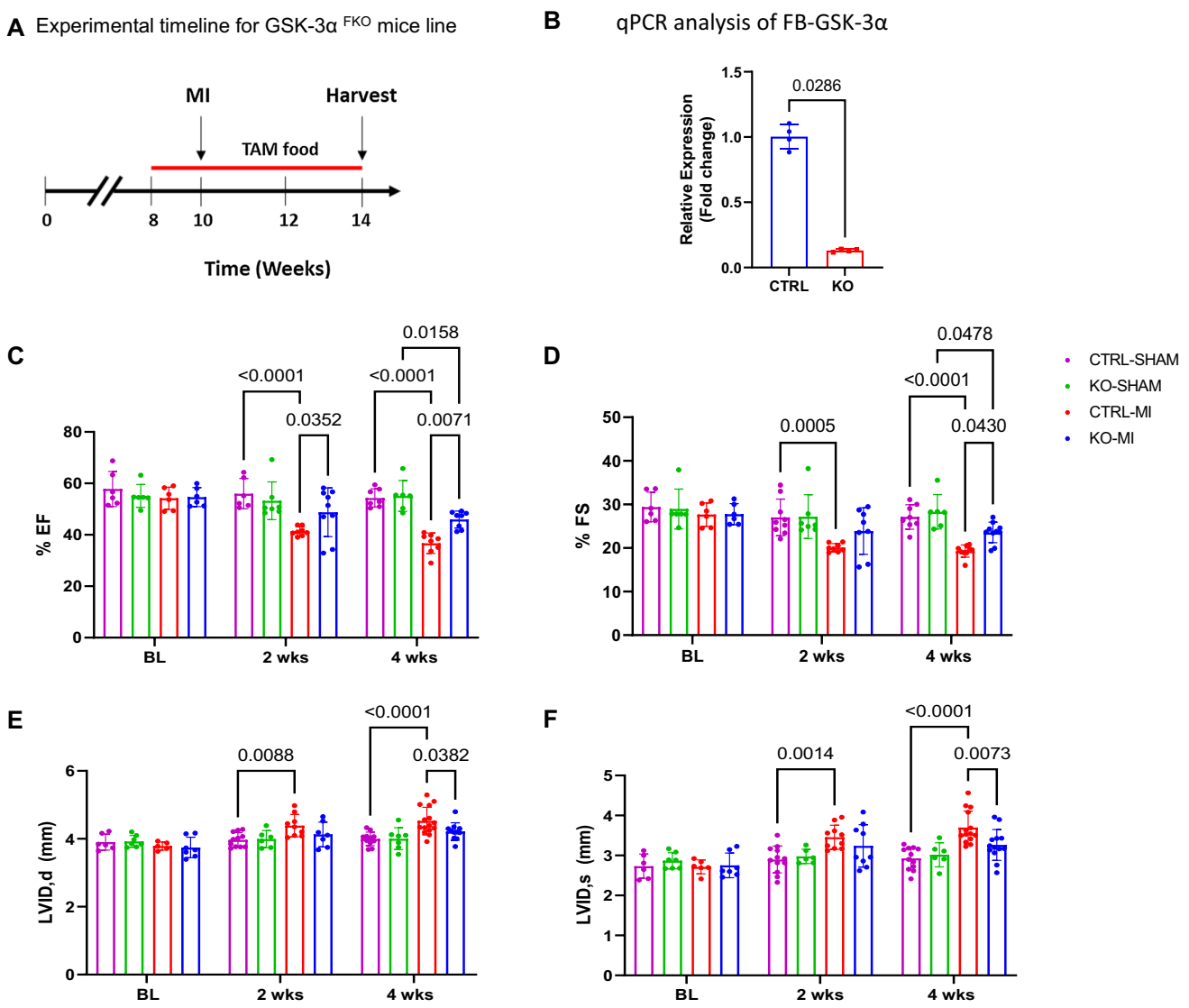

Fig. 1 Deleting GSK-3α from resident cardiac fibroblast before injury prevents ischemia-induced cardiac dysfunction. **A** Experimental design. Two-month-old mice were fed tamoxifen (TAM) chow diet. After 2 weeks of TAM treatment, mice were subjected to MI surgery and are maintained on the TAM diet till the end of the study. **B** Cardiac fibroblasts were isolated after TAM treatment to confirm the deletion. qPCR analysis of GSK-3α gene expression. Data were analyzed using the nonparametric Mann–Whitney test and represented as mean ± SD $N = 4$ per group. Evaluation of cardiac function by m-mode echocardiography; **C** Ejection fraction (EF), **D** Fractional shortening (FS), **E** LV end-diastolic interior dimension (LVID;d) and **F** LV end-systolic interior dimension (LVID;s). Data were analyzed using Two-way ANOVA followed by Tukey's post hoc analysis and represented as mean ± SD $N = 6$–10 per group. *BL* baseline

qPCR analysis confirmed significant upregulation in gene expression of pro-inflammatory cytokines (IL-1β, IL-6, and TNF-α). These molecular markers of chronic inflammation were essentially normalized due to FB-specific deletion of GSK-3α (Fig. 3A–C). GSK-3 has been implicated in inflammation associated with various diseases [9, 10, 19, 22, 30, 56]. Since NF-kB is the master regulator of the inflammatory response [16, 33] we examined the effect of GSK-3α deletion on NF-kB activation. WT and GSK-3α KO mouse embryonic fibroblasts (MEFs) were treated with TNF-α (10 ng/mL, 1 h), and NF-kB activation was assessed by analyzing p65 and IκBα levels. Western blot results showed that TNF-α-induced phosphorylation of p65 and downregulation of IκBα were prohibited in KO FBs (Fig. 3D–F). To further verify whether FB-GSK-3α can cross-talk with immune cells, co-culture experiments were set up. WT and GSK-3α KO FBs were co-cultured with splenocytes for 24 h. RNA was extracted from splenocytes, followed by gene expression analysis. Strikingly, immune cells co-cultured with KO FBs displayed significant downregulation in gene expression of pro-inflammatory cytokines (IL-1β, IL-6, and TNF-α) as compared to those cultured with WT FBs (Fig. 3G–I). To

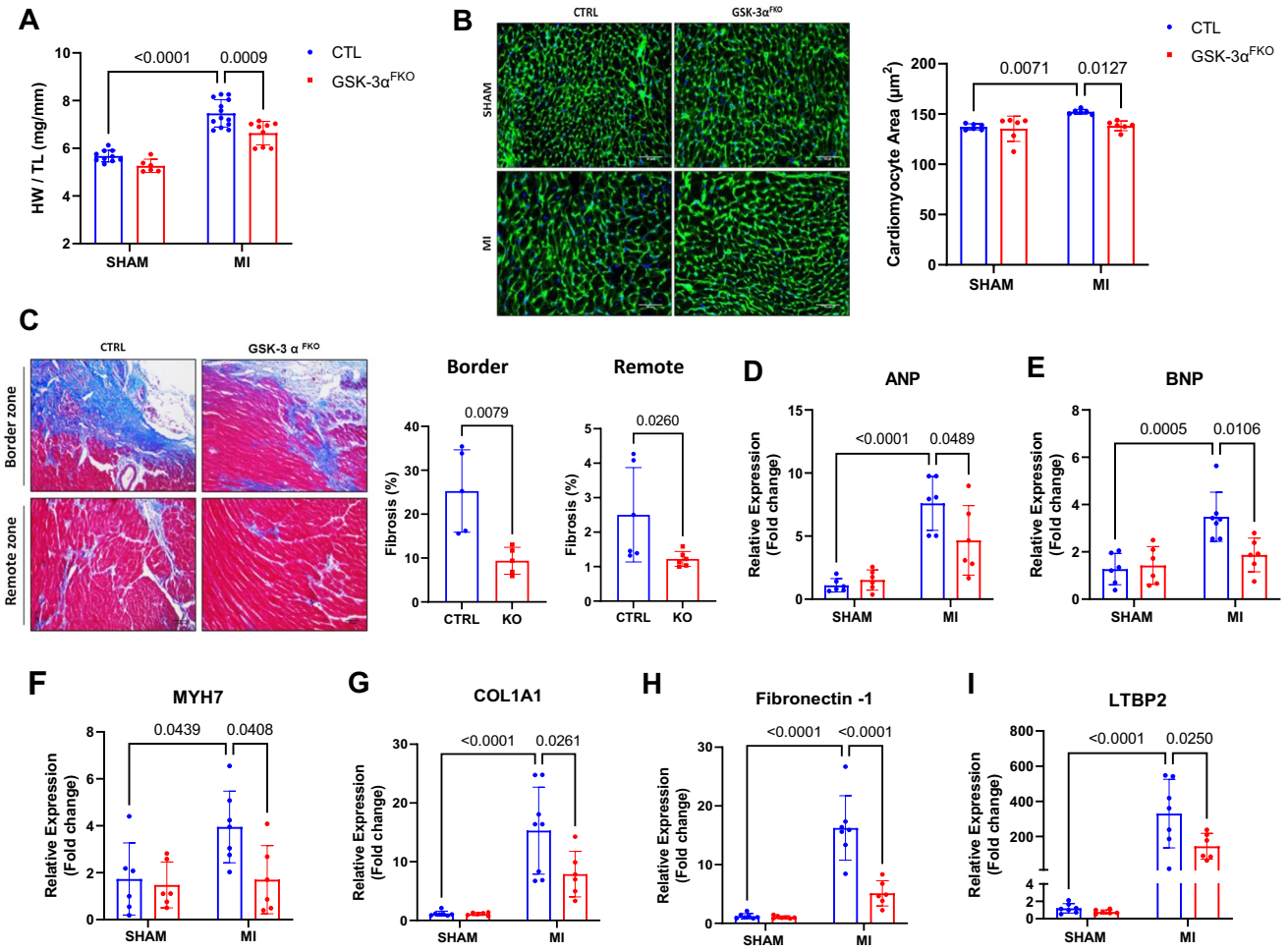

Fig. 2 FB-specific deletion of GSK-3α prevents ischemia-induced cardiac hypertrophy and fibrosis. Morphometric studies were performed at 4 weeks after MI surgery. Assessment of cardiac hypertrophy; **A** heart weight (HW) to tibia length (TL) ratio and **B** representative image of WGA-FITC stained heart sections and quantification of cardiomyocyte cross-sectional area (CSA). Scale bar = 50 µm. **C** Assessment of cardiac fibrosis by Masson's Trichrome staining; Representative Trichrome-stained LV regions and Quantification of LV fibrosis. Scale bar = 100 µm. At 4 weeks after MI surgery, RNA was extracted from the left ventricle of experimental animals, and gene expression analysis was carried out by qPCR; **D** ANP, **E** BNP, **F** MYH7, **G** COL1A1, **H** fibronectin-1, **I** Latent TGF-β binding protein 2 (LTBP-2). Data were analyzed using Two-way ANOVA followed by Tukey's post hoc analysis and represented as mean ± SD $N = 6–9$ per group

assess angiogenesis, capillary density was evaluated using CD31 staining. The analysis showed that capillary density is significantly improved in the KO-MI heart as compared to the CTRL-MI group (Fig. 3J). FBs are known to play a regulatory role in angiogenesis [36, 40, 43, 45]. Moreover, GSK-3β has been implicated with angiogenesis [24, 42, 47]. To examine whether GSK-3α deletion had any effect on angiogenesis-related proteins in FBs, we isolated cardiac FBs from experimental animals at 1-week post-MI and analyzed levels of 53 angiogenesis-related proteins using the proteome profiler (Fig. 3K). KO group displayed significant alteration in 6 key proteins (Amphiregulin, Hepatocyte Growth Factor, Serpin E1, platelet factor 4, MMP9, and ADAMTS1) that are known to regulate angiogenesis [5, 21, 28, 37, 44, 55].

Deleting GSK-3α from myofibroblast protects the heart from MI-induced cardiac dysfunction and remodeling

In the injured heart, the quiescent fibroblast gets transformed into an active fibroblast or myofibroblast. This FB population plays an important role in the healing and scar maturation phase post-MI. Thus, to examine the effect of myofibroblast-specific GSK-3α role in MI heart, we employed the Postn-MCM model. Myofibroblast-specific GSK-3α KO mice were generated as described previously [53]. Briefly, Postn-MCM mice were crossed with GSK-3$\alpha^{fl/fl}$ mice to obtain GSK-3$\alpha^{fl/fl}$/Postn-MCM$^{+/-}$ (KO) and GSK-3$\alpha^{fl/fl}$/Postn-MCM$^{-/-}$ (CTRL). Tamoxifen protocol was employed. After 1 week of tamoxifen treatment, mice

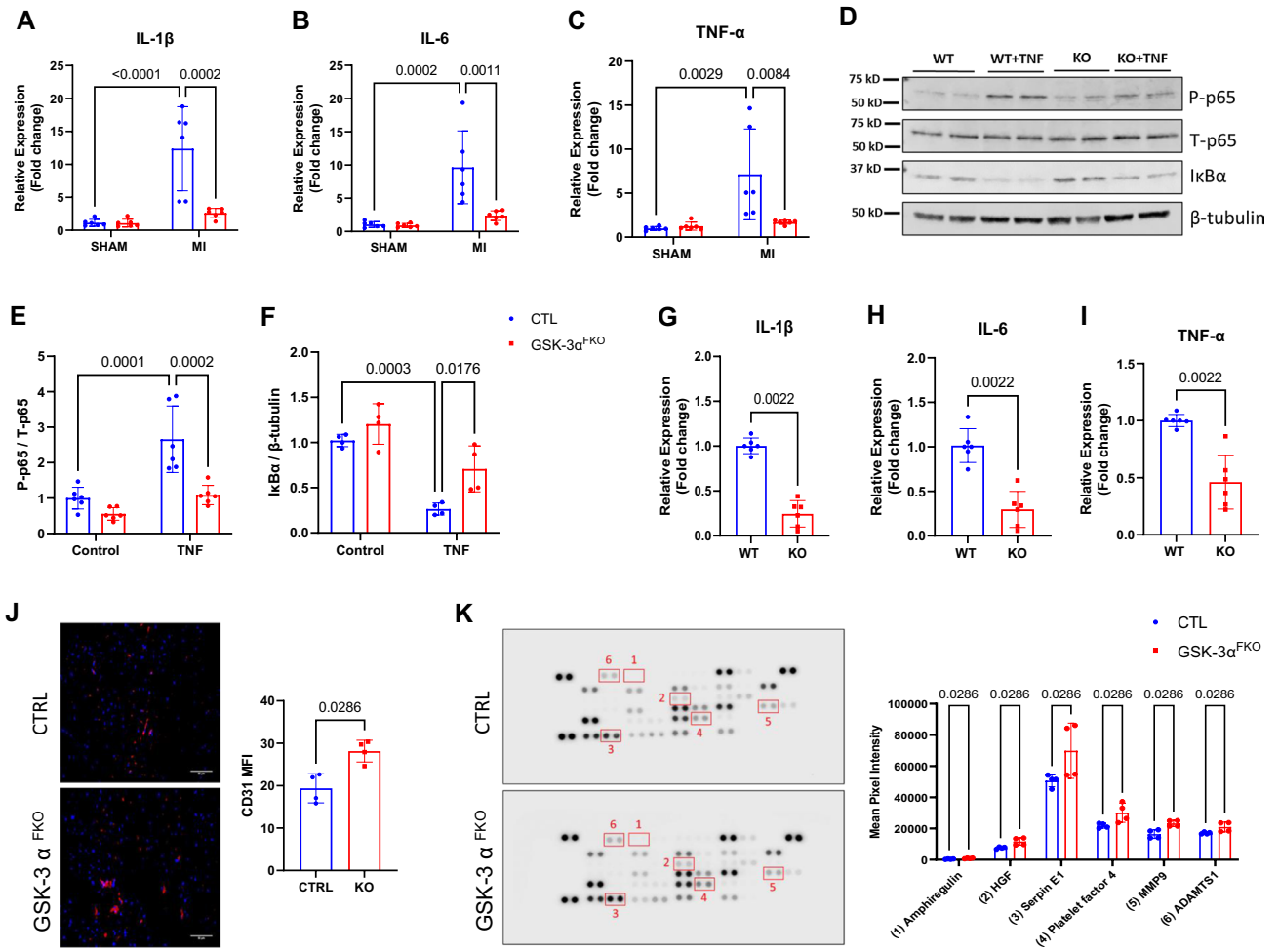

Fig. 3 Deletion of GSK-3α from resident cardiac fibroblasts reduces inflammation and promotes angiogenesis in the MI heart. At 4 weeks after MI surgery, RNA was extracted from the left ventricle of experimental animals, and gene expression analysis was carried out by qPCR; **A** IL-1β, **B** IL-6, **C** TNF-α. Data were analyzed using Two-way ANOVA followed by Tukey's post hoc analysis and represented as mean ± SD $N = 5–8$ per group. WT and KO MEFs were treated with TNF-α (10 ng/mL) for 1 h. Western blot analysis was performed to assess the activation NF-κB pathway. **D** Representative blot and quantification of **E** p65, **F** IkBα. Data were analyzed using Two-way ANOVA followed by Tukey's post hoc analysis and represented as mean ± SD $N = 4–6$. WT and KO MEFs were co-cultured with splenocytes for 24 h. After co-culturing, RNA was extracted from splenocytes, and gene expression analysis was carried out by qPCR; **G** IL-1β, **H** IL-6, **I** TNF-α. Data were analyzed using the nonparametric Mann–Whitney test and represented as mean ± SD $N = 6$ per group. **J** Representative images of CD31 staining and quantification of mean fluorescence intensity (MFI). Scale bar = 50 µm. Data were analyzed using the nonparametric Mann–Whitney test and represented as mean ± SD $N = 4$ per group. **K** Cardiac FBs were isolated from the heart of control and GSK-3 α^{FKO} mice at 1-week post-MI and proteins were analyzed using Mouse Angiogenesis Proteome Profiler Array. Representative blots and quantification of Mean Pixel Intensity. Data were analyzed using the nonparametric Mann–Whitney test and represented as mean ± SD $N = 4$ per group

were subjected to MI surgery. At 4 weeks post-MI, FBs were isolated from the hearts of the experimental animals, and gene expression analysis was carried out. The qPCR results confirmed a significant reduction in GSK-3α gene expression in KO FBs as compared to the control group (Fig. 4A and B). MI-induced mortality was comparable between the groups (data not shown). Analysis of cardiac function by echocardiography displayed improvement in EF and FS in the KO group (Fig. 4C and D). Moreover, LVIDs were remarkably normalized in the KO-MI group as compared to the controls (Fig. 4E and F). To further confirm cardioprotective phenotype in KO, we did morphometrics and histological studies at 4 weeks post MI. Analysis of HW/TL, CSA, and fibrosis revealed a significant reduction in these parameters in KO-MI mice compared to controls (Fig. 5A–C). Also, CD31 staining showed improvement in capillary density in KO hearts (Fig. 5D). Additionally, the expression of signature genes related to cardiac hypertrophy (ANP, BNP, and MYH7), fibrosis (COL1A1, COL3A1, and COMP), and chronic inflammation (IL-1β, IL-6, and TNF-α)

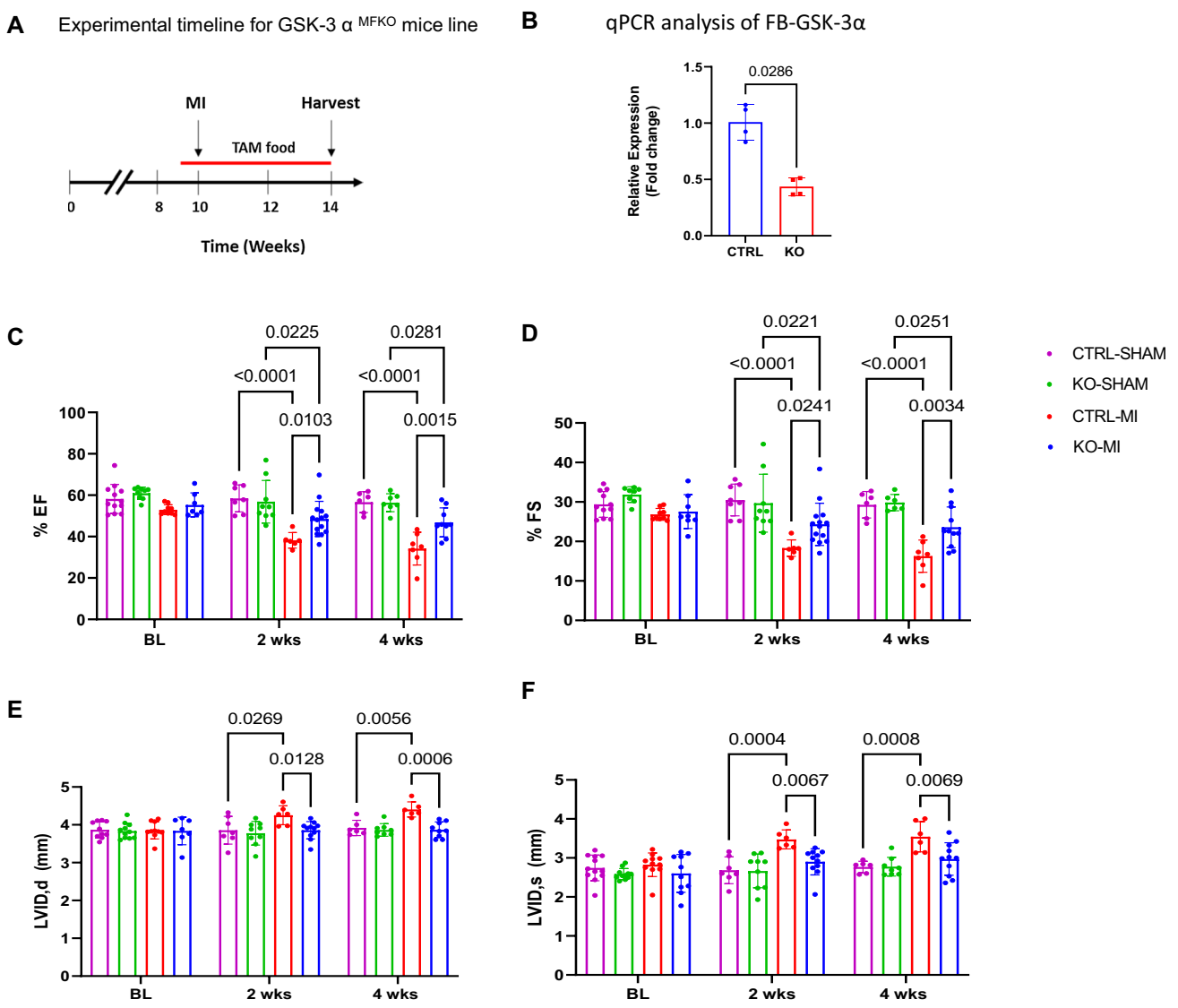

Fig. 4 Deleting GSK-3α from myofibroblast post-injury protects the heart from MI-induced cardiac dysfunction. **A** Experimental design. Two-month-old mice were fed tamoxifen (TAM) chow diet. After 1 week of TAM treatment, mice were subjected to MI surgery and are maintained on the TAM diet till the end of the study. **B** Cardiac fibroblasts were isolated after 4 weeks post-MI to confirm the GSK-3α deletion. qPCR analysis of GSK-3α gene expression. Data were analyzed using the nonparametric Mann–Whitney test and represented as mean ± SD $N = 4$ per group. Evaluation of cardiac function by m-mode echocardiography; **C** ejection fraction (EF), **D** fractional shortening (FS), **E** LV end-diastolic interior dimension (LVID;d) and **F** LV end-systolic interior dimension (LVID;s). Data were analyzed using Two-way ANOVA followed by Tukey's post hoc analysis and represented as mean ± SD $N = 5$–14 per group. *BL* baseline

was normalized after myofibroblast-specific GSK-3α deletion (Fig. 5E–M).

Discussion

Herein, we identify that FB-GSK-3α is a critical mediator of adverse cardiac remodeling and dysfunction of the ischemic heart. We employed advanced mouse models (Tcf21-MCM and Postn-MCM) to delete GSK-3α in FB specific manner and found that FB-specific GSK-3α deletion reduced excessive fibrosis and chronic inflammation, prevented dilative remodeling, and improved angiogenesis. While the cardiomyocyte proliferation was comparable between the groups (Supplemental Fig. 1), the FB-GSK-3α KOs hearts demonstrated a decreased MI-induced cardiomyocyte death compared to controls (Supplemental Fig. 2). Importantly, MI-induced functional decline was prohibited in KO mice. These observations confirmed that

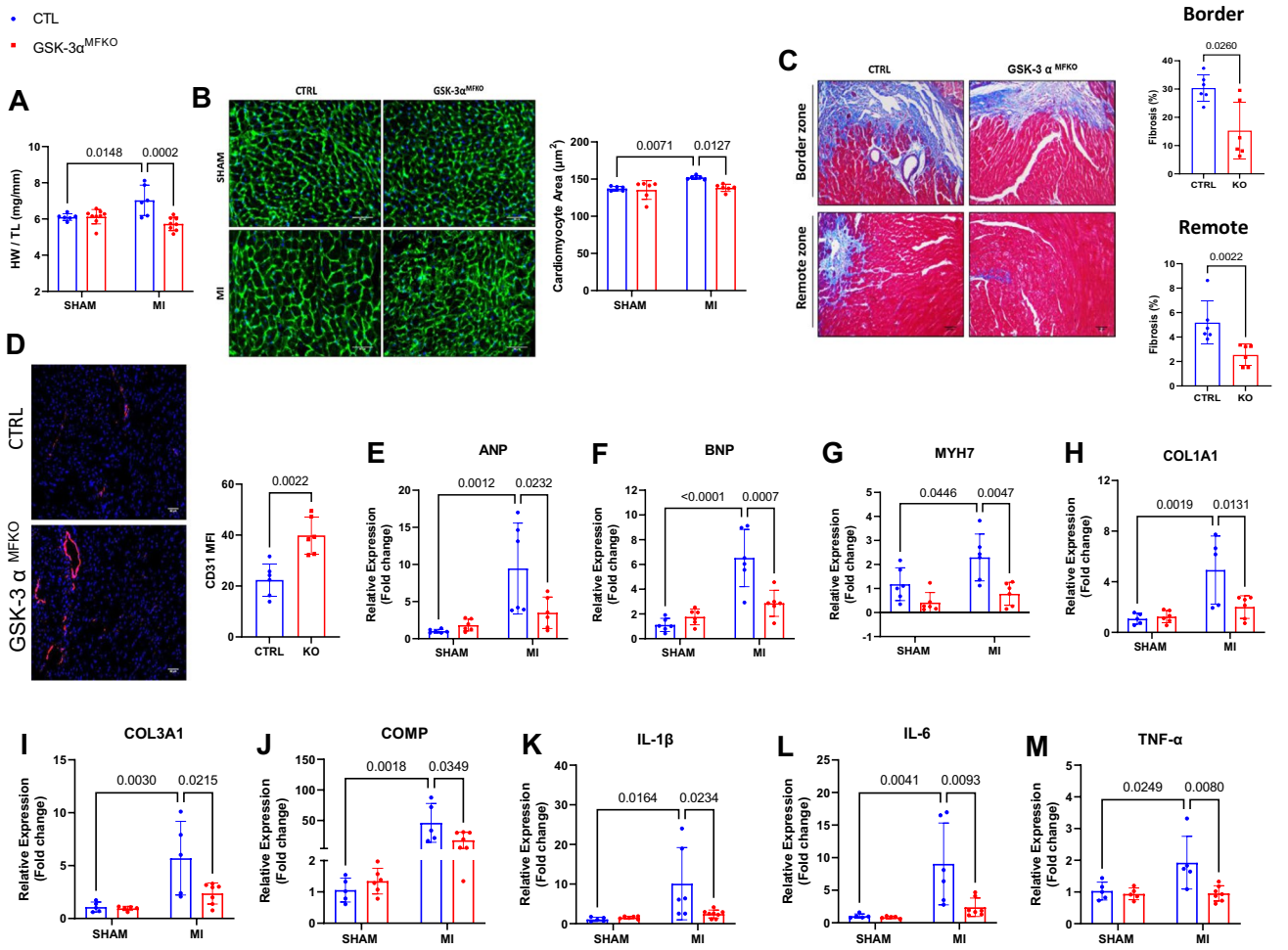

Fig. 5 Myofibroblast-specific deletion of GSK-3α prevents ischemia-induced adverse cardiac remodeling. Morphometric studies were performed at 4 weeks after MI surgery. Assessment of cardiac hypertrophy; **A** heart weight (HW) to tibia length (TL) ratio and **B** Representative image of WGA-FITC stained heart sections and quantification of cardiomyocyte cross-sectional area (CSA). Scale bar = 50 μm. **C** Assessment of cardiac fibrosis by Masson's trichrome staining; representative trichrome-stained LV regions and Quantification of LV fibrosis. Scale bar = 100 μm. **D** Representative images of CD31 staining and quantification of mean fluorescence intensity (MFI). Scale bar = 50 μm. Data were analyzed using the nonparametric Mann–Whitney test and represented as mean ± SD $N = 6$ per group. RNA was extracted from the left ventricle of experimental animals, and gene expression analysis was carried out by qPCR; **E** ANP, **F** BNP, **G** MYH7, **H** COL1A1, **I** COL3A1, **J** cartilage oligomeric matrix protein (COMP), **K** IL-1β, **L** IL-6, **M** TNF-α. Data were analyzed using Two-way ANOVA followed by Tukey's post hoc analysis and represented as mean ± SD. $N = 5$–9 per group

FB-GSK-3α plays a causal role in MI pathologies and represents a potential therapeutic target.

Previously our lab reported that global GSK-3α KOs developed spontaneous cardiac hypertrophy and dysfunction by 3–4 months of age [27]. Notably, When subjected to MI, global KO mice displayed significant mortality due to cardiac rupture. Studies from other groups have demonstrated that global embryonic GSK-3α KO leads to a detrimental phenotype [27, 58, 59]. We believe the reported detrimental phenotype in GSK-3α global KOs is primarily due to the developmental effects driven by embryonic GSK-3α deletion. The mechanism has been attributed to increased cardiomyocyte death, impaired autophagy, and accelerated aging [27, 58, 59]. In contrast to global GSK-3α KO, inhibition of GSK-3α in the adult heart (conditional) displayed cardioprotective phenotype in multiple settings [2, 3, 51, 53]. In line with these reports, we also observed that targeting FB-GSK-3α in adult mouse hearts offers benefits against MI-induced cardiac damage. The global embryonic vs. tissue-specific conditional GSK-3α targeting, associated cellular/molecular mechanisms, and phenotypic outcomes have been recently reviewed [51].

MI-triggered wound healing response and adaptive remodeling help to maintain cardiac function. However, disturbances in fine-tuning of cellular cross-talk perturb healing and cause adverse cardiac remodeling, subsequently leading to heart failure and mortality [8, 12, 38]. Thus a better understanding of the cellular and molecular basis of

ischemia-induced pathologies is of prime importance in developing effective therapeutic strategies. In the current study, we observed that FB-GSK-3α KO hearts had a significant reduction in the expression of inflammatory genes. Moreover, in vitro studies demonstrated that FB-GSK-3α is involved in NF-κB activation and modulation of inflammatory gene expression in immune cells. As per our knowledge, most of the studies that have shown the role of GSK-3 in inflammation were GSK-3β isoform centric [9, 10, 19, 22, 30, 56]. Herein, we present findings that suggest the potential role of FB-GSK-3α in modulating inflammatory signaling and cross-talk with immune cells. FBs and GSK-3 have also shown regulatory functions in angiogenesis [24, 36, 40, 42, 43, 45, 47]. Improved capillary density in the KO heart and alterations in the expression of angiogenesis-related proteins in KO FBs indicate that FB-GSK-3α might have a role in angiogenesis. Although these findings are promising, further studies are needed to discern how FB-GSK-3α mediates intercellular cross-talk and regulates angiogenesis/inflammation in the MI heart. Also, the exact molecular mechanism through which GSK-3α regulates NF-κB signaling and expression of angiogenesis-related proteins in FBs needs further investigation. Emerging studies have shown that in addition to phenotypic plasticity, fibroblasts exhibit remarkable heterogeneity [18, 29, 34, 54, 57]. Future single-cell sequencing studies are needed to identify the role of FB-GSK-3α in distinct fibroblast subsets that may be responsible for the wide range of functions in the injured heart.

We reported that FB-GSK-3β acts as a negative regulator of fibrosis in the ischemic heart [26]. Further mechanistic studies revealed that FB-GSK-3β directly interacts with SMAD3 and regulates classical TGFβ/SMAD3 signaling to inhibit MyoFB transformation and fibrosis in the ischemic heart. However, in stark contrast to the FB-GSK-3β role, FB-GSK-3α appears to contribute to adverse fibrotic remodeling in the pressure-overload model of heart failure [53]. FB-GSK-3α was found to promote fibrosis through the RAF-MEK-ERK pathway that operates independently of TGFβ/SMAD3 signaling. Importantly, targeting GSK-3α in an FB-specific manner prevented fibrosis and improved cardiac function in TAC mice. This contrasting role of GSK-3 isoforms in cardiac pathologies persuaded us to examine whether GSK-3α plays a unique role irrespective of the type of injury insult. We observed that FB-GSK-3α targeting helps to reduce fibrosis in the MI heart, thus validating its pro-fibrotic role in heart diseases with different etiologies. The beneficial effects of cell-specific targeting of GSK-3α have been reported earlier as well. For instance, Firdos et al. employed CM-specific conditional KO and identified that deletion of GSK-3α specifically from CM offers cardioprotection in rodent models of heart failure such as MI and TAC [2, 3]. Sadoshima's group demonstrated that CM-GSK-3α participates in lipotoxic cardiomyopathy and targeting GSK-3α in a CM-specific manner offers cardioprotection [39]. In line with all these emerging reports, our study demonstrates that GSK-3α has cell-specific unique mechanisms in the pathophysiology of cardiac disease. However, further investigation of clinical correlates of these experimental findings is needed to confirm translational potential.

In summary, our study reveals that FB-GSK-3α promotes adverse cardiac remodeling and dysfunction after MI. These findings pave the way for developing targeted therapy for managing heart diseases.

Supplementary Information The online version contains supplementary material available at https://doi.org/10.1007/s00395-023-01005-1.

Author contributions PU and HL conceived and designed the research; PU, SR, SE, and ST performed experiments; PU, SR, and SE analyzed data; PU, ST, and HL interpreted results of experiments; PU prepared figures; PU and HL drafted the manuscript; all authors contributed to editing, revision, and approved the final version of the manuscript.

Funding This work was supported by research grants from the NHLBI (R01HL133290 and 1R01HL143074) to HL, American Heart Association (AHA CDA 933553) to ST.

Data availability Data will be made available upon reasonable request.

Declarations

Conflict of interest The authors have no conflicting interests to disclose in relation to this work.

References

1. Acharya A, Baek ST, Huang G, Eskiocak B, Goetsch S, Sung CY, Banfi S, Sauer MF, Olsen GS, Duffield JS, Olson EN, Tallquist MD (2012) The bHLH transcription factor Tcf21 is required for lineage-specific EMT of cardiac fibroblast progenitors. Development 139:2139–2149. https://doi.org/10.1242/dev.079970
2. Ahmad F, Lal H, Zhou J, Vagnozzi RJ, Yu JE, Shang X, Woodgett JR, Gao E, Force T (2014) Cardiomyocyte-specific deletion of Gsk3alpha mitigates post-myocardial infarction remodeling, contractile dysfunction, and heart failure. J Am Coll Cardiol 64:696–706. https://doi.org/10.1016/j.jacc.2014.04.068
3. Ahmad F, Singh AP, Tomar D, Rahmani M, Zhang Q, Woodgett JR, Tilley DG, Lal H, Force T (2019) Cardiomyocyte-GSK-3alpha promotes mPTP opening and heart failure in mice with chronic pressure overload. J Mol Cell Cardiol 130:65–75. https://doi.org/10.1016/j.yjmcc.2019.03.020
4. Ahmad F, Woodgett JR (2020) Emerging roles of GSK-3alpha in pathophysiology: emphasis on cardio-metabolic disorders. Biochim Biophys Acta Mol Cell Res 1867:118616. https://doi.org/10.1016/j.bbamcr.2019.118616
5. Bergers G, Brekken R, McMahon G, Vu TH, Itoh T, Tamaki K, Tanzawa K, Thorpe P, Itohara S, Werb Z, Hanahan D (2000) Matrix metalloproteinase-9 triggers the angiogenic switch during carcinogenesis. Nat Cell Biol 2:737–744. https://doi.org/10.1038/35036374
6. Brauninger H, Kruger S, Bacmeister L, Nystrom A, Eyerich K, Westermann D, Lindner D (2023) Matrix metalloproteinases in coronary artery disease and myocardial infarction. Basic Res Cardiol 118:18. https://doi.org/10.1007/s00395-023-00987-2

7. Brooks HL, Lindsey ML (2018) Guidelines for authors and reviewers on antibody use in physiology studies. Am J Physiol Heart Circ Physiol 314:H724–H732. https://doi.org/10.1152/ajpheart.00512.2017
8. Chalise U, Becirovic-Agic M, Lindsey ML (2023) The cardiac wound healing response to myocardial infarction. WIREs Mech Dis 15:e1584. https://doi.org/10.1002/wsbm.1584
9. Cinetto F, Ceccato J, Caputo I, Cangiano D, Montini B, Lunardi F, Piazza M, Agostini C, Calabrese F, Semenzato G, Rattazzi M, Gurrieri C, Scarpa R, Felice C, Vianello F (2021) GSK-3 inhibition modulates metalloproteases in a model of lung inflammation and fibrosis. Front Mol Biosci 8:633054. https://doi.org/10.3389/fmolb.2021.633054
10. Cortes-Vieyra R, Silva-Garcia O, Gomez-Garcia A, Gutierrez-Castellanos S, Alvarez-Aguilar C, Baizabal-Aguirre VM (2021) Glycogen synthase kinase 3beta modulates the inflammatory response activated by bacteria, viruses, and parasites. Front Immunol 12:675751. https://doi.org/10.3389/fimmu.2021.675751
11. Doble BW, Patel S, Wood GA, Kockeritz LK, Woodgett JR (2007) Functional redundancy of GSK-3alpha and GSK-3beta in Wnt/beta-catenin signaling shown by using an allelic series of embryonic stem cell lines. Dev Cell 12:957–971. https://doi.org/10.1016/j.devcel.2007.04.001
12. Frangogiannis NG (2006) The mechanistic basis of infarct healing. Antioxid Redox Signal 8:1907–1939. https://doi.org/10.1089/ars.2006.8.1907
13. Frangogiannis NG (2015) Pathophysiology of myocardial infarction. Compr Physiol 5:1841–1875. https://doi.org/10.1002/cphy.c150006
14. Fu X, Khalil H, Kanisicak O, Boyer JG, Vagnozzi RJ, Maliken BD, Sargent MA, Prasad V, Valiente-Alandi I, Blaxall BC, Molkentin JD (2018) Specialized fibroblast differentiated states underlie scar formation in the infarcted mouse heart. J Clin Investig 128:2127–2143. https://doi.org/10.1172/JCI98215
15. Gao E, Lei YH, Shang X, Huang ZM, Zuo L, Boucher M, Fan Q, Chuprun JK, Ma XL, Koch WJ (2010) A novel and efficient model of coronary artery ligation and myocardial infarction in the mouse. Circ Res 107:1445–1453. https://doi.org/10.1161/CIRCRESAHA.110.223925
16. Ghosh S, Hayden MS (2008) New regulators of NF-kappaB in inflammation. Nat Rev Immunol 8:837–848. https://doi.org/10.1038/nri2423
17. Hess A, Borchert T, Ross TL, Bengel FM, Thackeray JT (2022) Characterizing the transition from immune response to tissue repair after myocardial infarction by multiparametric imaging. Basic Res Cardiol 117:14. https://doi.org/10.1007/s00395-022-00922-x
18. Hesse J, Owenier C, Lautwein T, Zalfen R, Weber JF, Ding Z, Alter C, Lang A, Grandoch M, Gerdes N, Fischer JW, Klau GW, Dieterich C, Kohrer K, Schrader J (2021) Single-cell transcriptomics defines heterogeneity of epicardial cells and fibroblasts within the infarcted murine heart. Elife. https://doi.org/10.7554/eLife.65921
19. Hoffmeister L, Diekmann M, Brand K, Huber R (2020) GSK3: a kinase balancing promotion and resolution of inflammation. Cells. https://doi.org/10.3390/cells9040820
20. Humeres C, Frangogiannis NG (2019) Fibroblasts in the infarcted, remodeling, and failing heart. JACC Basic Transl Sci 4:449–467. https://doi.org/10.1016/j.jacbts.2019.02.006
21. Isogai C, Laug WE, Shimada H, Declerck PJ, Stins MF, Durden DL, Erdreich-Epstein A, DeClerck YA (2001) Plasminogen activator inhibitor-1 promotes angiogenesis by stimulating endothelial cell migration toward fibronectin. Cancer Res 61:5587–5594
22. Jope RS, Cheng Y, Lowell JA, Worthen RJ, Sitbon YH, Beurel E (2017) Stressed and inflamed, can GSK3 be blamed? Trends Biochem Sci 42:180–192. https://doi.org/10.1016/j.tibs.2016.10.009
23. Kanisicak O, Khalil H, Ivey MJ, Karch J, Maliken BD, Correll RN, Brody MJ, Lin S-CJ, Aronow BJ, Tallquist MD, Molkentin JD (2016) Genetic lineage tracing defines myofibroblast origin and function in the injured heart. Nat Commun 7:12260. https://doi.org/10.1038/ncomms12260
24. Kim HS, Skurk C, Thomas SR, Bialik A, Suhara T, Kureishi Y, Birnbaum M, Keaney JF Jr, Walsh K (2002) Regulation of angiogenesis by glycogen synthase kinase-3beta. J Biol Chem 277:41888–41896. https://doi.org/10.1074/jbc.M206657200
25. Lal H, Ahmad F, Woodgett J, Force T (2015) The GSK-3 family as therapeutic target for myocardial diseases. Circ Res 116:138–149. https://doi.org/10.1161/CIRCRESAHA.116.303613
26. Lal H, Ahmad F, Zhou J, Yu JE, Vagnozzi RJ, Guo Y, Yu D, Tsai EJ, Woodgett J, Gao E, Force T (2014) Cardiac fibroblast glycogen synthase kinase-3beta regulates ventricular remodeling and dysfunction in ischemic heart. Circulation 130:419–430. https://doi.org/10.1161/CIRCULATIONAHA.113.008364
27. Lal H, Zhou J, Ahmad F, Zaka R, Vagnozzi RJ, Decaul M, Woodgett J, Gao E, Force T (2012) Glycogen synthase kinase-3alpha limits ischemic injury, cardiac rupture, post-myocardial infarction remodeling and death. Circulation 125:65–75. https://doi.org/10.1161/CIRCULATIONAHA.111.050666
28. Lee NV, Sato M, Annis DS, Loo JA, Wu L, Mosher DF, Iruela-Arispe ML (2006) ADAMTS1 mediates the release of antiangiogenic polypeptides from TSP1 and 2. EMBO J 25:5270–5283. https://doi.org/10.1038/sj.emboj.7601400
29. Lendahl U, Muhl L, Betsholtz C (2022) Identification, discrimination and heterogeneity of fibroblasts. Nat Commun 13:3409. https://doi.org/10.1038/s41467-022-30633-9
30. Li Z, Zhu H, Liu C, Wang Y, Wang D, Liu H, Cao W, Hu Y, Lin Q, Tong C, Lu M, Sachinidis A, Li L, Peng L (2019) GSK-3beta inhibition protects the rat heart from the lipopolysaccharide-induced inflammation injury via suppressing FOXO3A activity. J Cell Mol Med 23:7796–7809. https://doi.org/10.1111/jcmm.14656
31. Lindsey ML, Bolli R, Canty JM Jr, Du XJ, Frangogiannis NG, Frantz S, Gourdie RG, Holmes JW, Jones SP, Kloner RA, Lefer DJ, Liao R, Murphy E, Ping P, Przyklenk K, Recchia FA, Schwartz Longacre L, Ripplinger CM, Van Eyk JE, Heusch G (2018) Guidelines for experimental models of myocardial ischemia and infarction. Am J Physiol Heart Circ Physiol 314:H812–H838. https://doi.org/10.1152/ajpheart.00335.2017
32. Lindsey ML, Kassiri Z, Virag JAI, de Castro Bras LE, Scherrer-Crosbie M (2018) Guidelines for measuring cardiac physiology in mice. Am J Physiol Heart Circ Physiol 314:H733–H752. https://doi.org/10.1152/ajpheart.00339.2017
33. Liu T, Zhang L, Joo D, Sun SC (2017) NF-kappaB signaling in inflammation. Signal Transduct Target Ther 2:17023. https://doi.org/10.1038/sigtrans.2017.23
34. Lother A, Kohl P (2023) The heterocellular heart: identities, interactions, and implications for cardiology. Basic Res Cardiol 118:30. https://doi.org/10.1007/s00395-023-01000-6
35. Ma Y, Iyer RP, Jung M, Czubryt MP, Lindsey ML (2017) Cardiac fibroblast activation post-myocardial infarction: current knowledge gaps. Trends Pharmacol Sci 38:448–458. https://doi.org/10.1016/j.tips.2017.03.001
36. Martin TA, Harding KG, Jiang WG (1999) Regulation of angiogenesis and endothelial cell motility by matrix-bound fibroblasts. Angiogenesis 3:69–76. https://doi.org/10.1023/a:1009004212357
37. Maurer AM, Zhou B, Han ZC (2006) Roles of platelet factor 4 in hematopoiesis and angiogenesis. Growth Factors 24:242–252. https://doi.org/10.1080/08977190600988225
38. Mouton AJ, Rivera OJ, Lindsey ML (2018) Myocardial infarction remodeling that progresses to heart failure: a signaling

misunderstanding. Am J Physiol Heart Circ Physiol 315:H71–H79. https://doi.org/10.1152/ajpheart.00131.2018
39. Nakamura M, Liu T, Husain S, Zhai P, Warren JS, Hsu CP, Matsuda T, Phiel CJ, Cox JE, Tian B, Li H, Sadoshima J (2019) Glycogen synthase kinase-3alpha promotes fatty acid uptake and lipotoxic cardiomyopathy. Cell Metab 29:1119-1134.e1112. https://doi.org/10.1016/j.cmet.2019.01.005
40. Newman AC, Nakatsu MN, Chou W, Gershon PD, Hughes CC (2011) The requirement for fibroblasts in angiogenesis: fibroblast-derived matrix proteins are essential for endothelial cell lumen formation. Mol Biol Cell 22:3791–3800. https://doi.org/10.1091/mbc.E11-05-0393
41. Percie du Sert N, Hurst V, Ahluwalia A, Alam S, Avey MT, Baker M, Browne WJ, Clark A, Cuthill IC, Dirnagl U, Emerson M, Garner P, Holgate ST, Howells DW, Karp NA, Lazic SE, Lidster K, MacCallum CJ, Macleod M, Pearl EJ, Petersen OH, Rawle F, Reynolds P, Rooney K, Sena ES, Silberberg SD, Steckler T, Wurbel H (2020) The ARRIVE guidelines 2.0: updated guidelines for reporting animal research. J Physiol 598:3793–3801. https://doi.org/10.1113/JP280389
42. Potz BA, Sabe AA, Elmadhun NY, Clements RT, Robich MP, Sodha NR, Sellke FW (2016) Glycogen synthase kinase 3beta inhibition improves myocardial angiogenesis and perfusion in a swine model of metabolic syndrome. J Am Heart Assoc. https://doi.org/10.1161/JAHA.116.003694
43. Saraswati S, Marrow SMW, Watch LA, Young PP (2019) Identification of a pro-angiogenic functional role for FSP1-positive fibroblast subtype in wound healing. Nat Commun 10:3027. https://doi.org/10.1038/s41467-019-10965-9
44. Sengupta S, Gherardi E, Sellers LA, Wood JM, Sasisekharan R, Fan TP (2003) Hepatocyte growth factor/scatter factor can induce angiogenesis independently of vascular endothelial growth factor. Arterioscler Thromb Vasc Biol 23:69–75. https://doi.org/10.1161/01.atv.0000048701.86621.d0
45. Shams F, Moravvej H, Hosseinzadeh S, Mostafavi E, Bayat H, Kazemi B, Bandehpour M, Rostami E, Rahimpour A, Moosavian H (2022) Overexpression of VEGF in dermal fibroblast cells accelerates the angiogenesis and wound healing function: in vitro and in vivo studies. Sci Rep 12:18529. https://doi.org/10.1038/s41598-022-23304-8
46. Shinde AV, Frangogiannis NG (2014) Fibroblasts in myocardial infarction: a role in inflammation and repair. J Mol Cell Cardiol 70:74–82. https://doi.org/10.1016/j.yjmcc.2013.11.015
47. Skurk C, Maatz H, Rocnik E, Bialik A, Force T, Walsh K (2005) Glycogen-Synthase Kinase3beta/beta-catenin axis promotes angiogenesis through activation of vascular endothelial growth factor signaling in endothelial cells. Circ Res 96:308–318. https://doi.org/10.1161/01.RES.0000156273.30274.f7
48. Tallquist MD, Molkentin JD (2017) Redefining the identity of cardiac fibroblasts. Nat Rev Cardiol 14:484–491. https://doi.org/10.1038/nrcardio.2017.57
49. Tsao CW, Aday AW, Almarzooq ZI, Anderson CAM, Arora P, Avery CL, Baker-Smith CM, Beaton AZ, Boehme AK, Buxton AE, Commodore-Mensah Y, Elkind MSV, Evenson KR, Eze-Nliam C, Fugar S, Generoso G, Heard DG, Hiremath S, Ho JE, Kalani R, Kazi DS, Ko D, Levine DA, Liu J, Ma J, Magnani JW, Michos ED, Mussolino ME, Navaneethan SD, Parikh NI, Poudel R, Rezk-Hanna M, Roth GA, Shah NS, St-Onge MP, Thacker EL, Virani SS, Voeks JH, Wang NY, Wong ND, Wong SS, Yaffe K, Martin SS, American Heart Association Council on E, Prevention Statistics C, Stroke Statistics S (2023) Heart disease and stroke statistics—2023 update: a report from the American Heart Association. Circulation 147:e93–e621. https://doi.org/10.1161/CIR.0000000000001123
50. Umbarkar P, Ejantkar S, Tousif S, Lal H (2021) Mechanisms of fibroblast activation and myocardial fibrosis: lessons learned from FB-specific conditional mouse models. Cells. https://doi.org/10.3390/cells10092412
51. Umbarkar P, Ruiz Ramirez SY, Toro Cora A, Tousif S, Lal H (2023) GSK-3 at the heart of cardiometabolic diseases: Isoform-specific targeting is critical to therapeutic benefit. Biochim Biophys Acta Mol Basis Dis 1869:166724. https://doi.org/10.1016/j.bbadis.2023.166724
52. Umbarkar P, Singh AP, Gupte M, Verma VK, Galindo CL, Guo Y, Zhang Q, McNamara JW, Force T, Lal H (2019) Cardiomyocyte SMAD4-dependent TGF-beta signaling is essential to maintain adult heart homeostasis. JACC Basic Transl Sci 4:41–53. https://doi.org/10.1016/j.jacbts.2018.10.003
53. Umbarkar P, Tousif S, Singh AP, Anderson JC, Zhang Q, Tallquist MD, Woodgett J, Lal H (2022) Fibroblast GSK-3alpha promotes fibrosis via RAF-MEK-ERK pathway in the injured heart. Circ Res 131:620–636. https://doi.org/10.1161/CIRCRESAHA.122.321431
54. Vidal R, Wagner JUG, Braeuning C, Fischer C, Patrick R, Tombor L, Muhly-Reinholz M, John D, Kliem M, Conrad T, Guimaraes-Camboa N, Harvey R, Dimmeler S, Sauer S (2019) Transcriptional heterogeneity of fibroblasts is a hallmark of the aging heart. JCI Insight. https://doi.org/10.1172/jci.insight.131092
55. Wang CQ, Huang YW, Wang SW, Huang YL, Tsai CH, Zhao YM, Huang BF, Xu GH, Fong YC, Tang CH (2017) Amphiregulin enhances VEGF-A production in human chondrosarcoma cells and promotes angiogenesis by inhibiting miR-206 via FAK/c-Src/PKCdelta pathway. Cancer Lett 385:261–270. https://doi.org/10.1016/j.canlet.2016.10.010
56. Wang L, Wang Y, Zhang C, Li J, Meng Y, Dou M, Noguchi CT, Di L (2018) Inhibiting glycogen synthase kinase 3 reverses obesity-induced white adipose tissue inflammation by regulating apoptosis inhibitor of macrophage/CD5L-mediated macrophage migration. Arterioscler Thromb Vasc Biol 38:2103–2116. https://doi.org/10.1161/ATVBAHA.118.311363
57. Wang L, Yang Y, Ma H, Xie Y, Xu J, Near D, Wang H, Garbutt T, Li Y, Liu J, Qian L (2022) Single-cell dual-omics reveals the transcriptomic and epigenomic diversity of cardiac non-myocytes. Cardiovasc Res 118:1548–1563. https://doi.org/10.1093/cvr/cvab134
58. Zhou J, Freeman TA, Ahmad F, Shang X, Mangano E, Gao E, Farber J, Wang Y, Ma XL, Woodgett J, Vagnozzi RJ, Lal H, Force T (2013) GSK-3alpha is a central regulator of age-related pathologies in mice. J Clin Investig 123:1821–1832. https://doi.org/10.1172/JCI64398
59. Zhou J, Lal H, Chen X, Shang X, Song J, Li Y, Kerkela R, Doble BW, MacAulay K, DeCaul M, Koch WJ, Farber J, Woodgett J, Gao E, Force T (2010) GSK-3alpha directly regulates beta-adrenergic signaling and the response of the heart to hemodynamic stress in mice. J Clin Investig 120:2280–2291. https://doi.org/10.1172/JCI41407